Supplement of Hydrol. Earth Syst. Sci., 27, 969–990, 2023
https://doi.org/10.5194/hess-27-969-2023-supplement


Hydrology and Earth System Sciences
Open Access
EGU

*Supplement of*

# Controls on flood managed aquifer recharge through a heterogeneous vadose zone: hydrologic modeling at a site characterized with surface geophysics

**Zach Perzan et al.**

*Correspondence to:* Zach Perzan (zperzan@stanford.edu)

**Supplementary material**

This supplementary material includes a brief discussion of the impact of discretization scheme of root zone saturation (section 1), 2 additional tables (section 2) and 10 additional figures (section 3).

## 1 Root zone discretization

The simulations presented in the main text used a discretization scheme that represents the root zone as a single, meter-thick layer of model cells. To investigate the impact of this discretization scheme on root zone residence time, we performed additional simulations that discretized the upper meter of the model domain into 8 separate layers (in order from top to bottom: 0.05, 0.05, 0.15, 0.15, 0.15, 0.15, 0.15, and 0.15 m thick). This discretization scheme causes a significant increase in computational time, so we are unable to use it across all simulations. To choose four representative simulations to re-run with this discretization scheme, we first ranked all successful simulations by mean flood-MAR infiltration rate. We then randomly chose one simulation from each infiltration rate quartile (i.e., one with mean infiltration rate between the 0 and 25th percentile, one between the 25th and 50th percentile, etc.). For each of the four simulations, the eight root zone model layers were assigned the same coarse fraction values as in the original simulation and parameterized as described in section 3.3.2 in the main text.

The coarse discretization scheme used in the main text results in average root zone saturation errors between 3.49 and 5.58% (Table S1). However, the largest errors were localized to coarse-grained sediments (Fig. S7). Given that coarse-grained root zone sediments rarely exceed the 48-hour saturation threshold (Fig. 4 and Fig. S9), this simplified discretization scheme is unlikely to impact root zone saturation risk maps (e.g., Fig. 4b). As discussed in the section 6 in the main text, root zone heterogeneity not captured by the tTEM system likely constitutes a larger source of uncertainty than root zone discretization scheme.

## 2 Tables

**Table S1.** Effect of root zone discretization on root zone saturation following flood-MAR.

| Time since inundation | Mean absolute percentage error |
|---|---|
| 0–2 days | 5.58% |
| 0–7 days | 5.82% |
| 0–14 days | 5.82% |
| 0–30 days | 4.48% |
| 0–45 days | 3.49% |

Each value represents the mean absolute percentage error (MAPE) between the root zone saturation of the original simulation and the depth-averaged root zone saturation of that simulation re-run with a finer discretization scheme. MAPE values are averaged across four representative simulations.

## 3 Figures

**Table S2.** Effect of domain size on errors in subsurface storage and outcomes of interest.

| | | Subsurface storage error | | Errors in outcomes of interest | | |
|---|---|---|---|---|---|---|
| Padding | # of cells | Spinup | Inundation | Infiltration | RZ res. time | Recharge pct. |
| 200 m | 240,000 | -0.21% | -0.22% | 0.00% | 0.00% | 10.4% |
| 500 m | 630,000 | -0.14% | -0.15% | 0.00% | 0.00% | 3.8% |
| 700 m | 990,000 | -0.10% | -0.10% | 0.00% | 0.00% | 3.2% |
| 1000 m | 1,680,000 | N/A | N/A | N/A | N/A | N/A |

Each value represents the percent difference between a given simulation and the simulation run with 1000 m of padding. Subsurface storage errors represent the difference in total subsurface storage for a volume extending 100 m around the orchard and to the bottom of the model domain.

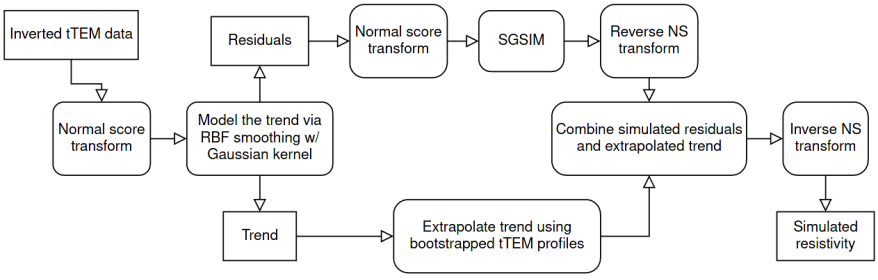


**Figure S1.** The full geostatistical workflow used to interpolate and extrapolate an inversion of the tTEM data onto a rectilinear grid. First, the resistivity model is transformed to a Gaussian distribution via rank transformation. Next, the trend is modeled using a radial basis function (RBF) with Gaussian kernel and values are decomposed into trend and residual components. Sequential Gaussian simulation (SGSIM) is then used to generate realizations of the stationary residuals. The trend is extrapolated using bootstrapped 1D profiles from within the domain (section 3.2.2), combined with the realizations of the residuals. Finally, the residuals and trend are added together and inverse transformed.

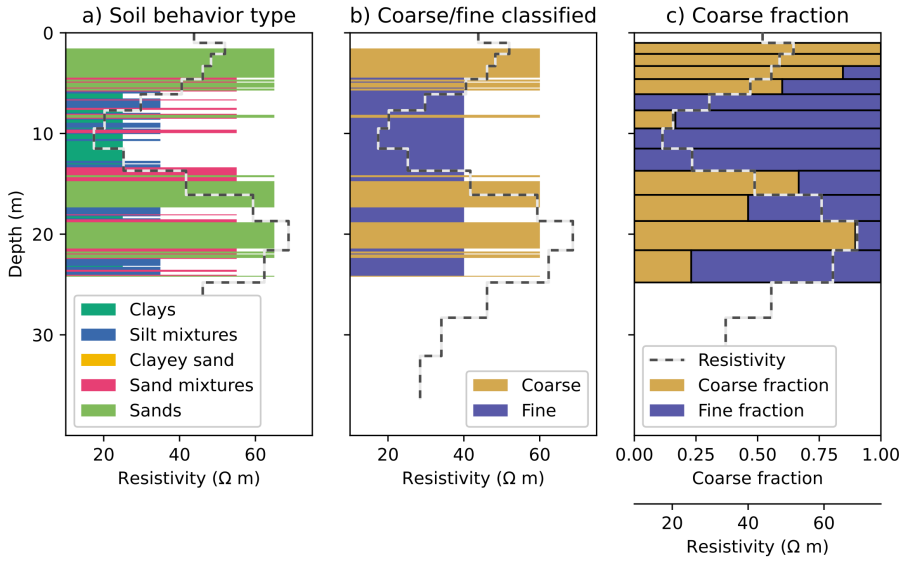


**Figure S2.** An example cone penetration test (CPT) log used to develop the resistivity-lithology model for transforming resistivity to coarse fraction. Normalized soil behavior types from each CPT depth interval (a) are classified as either fine- or coarse-grained (b). The classified logs are then upsampled to the resolution of the tTEM resistivity model (c) by calculating the percent of coarse-grained CPT observations within each tTEM pixel. Resistivity from the nearest inverted tTEM sounding is plotted in black and white over each log. The CPT logging interval was 10 cm.

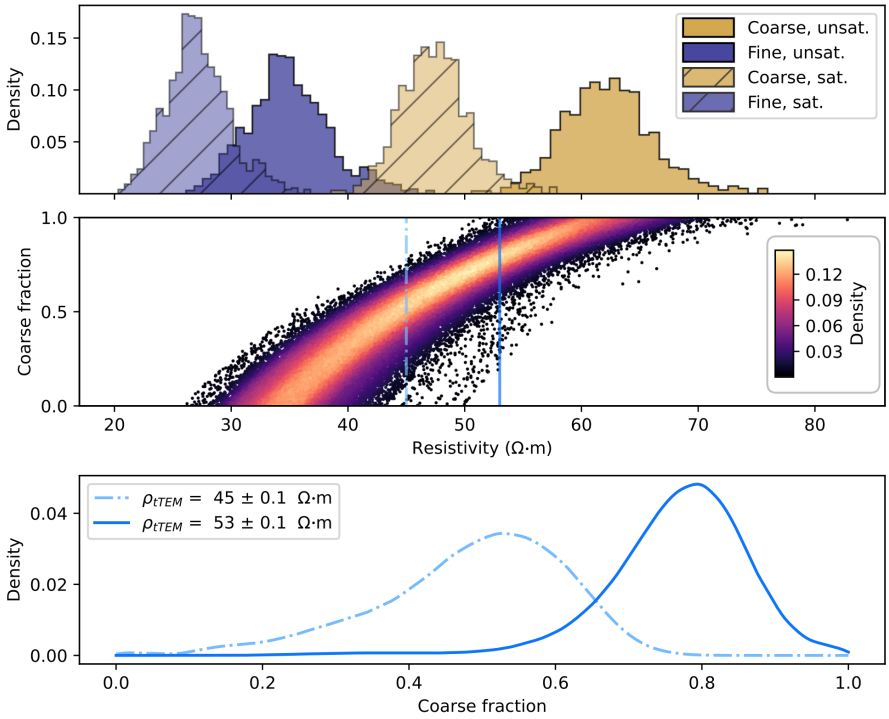


**Figure S3.** Resistivity-coarse fraction relationships used to create the rock physics transform. First, distributions of the expected resistivity values for coarse- and fine-grained end members (a) are generated from collocated cone penetration test (CPT) logs and tTEM soundings. We then sample from each distribution and use equation 2 in the main text to calculate paired coarse fraction and resistivity values (b). This process is performed separately for the unsaturated and saturated zones, though only the relationship for the unsaturated zone is plotted here. We then calculate the distribution of coarse fraction values in a series of discrete resistivity bins, two of which are plotted in (c).

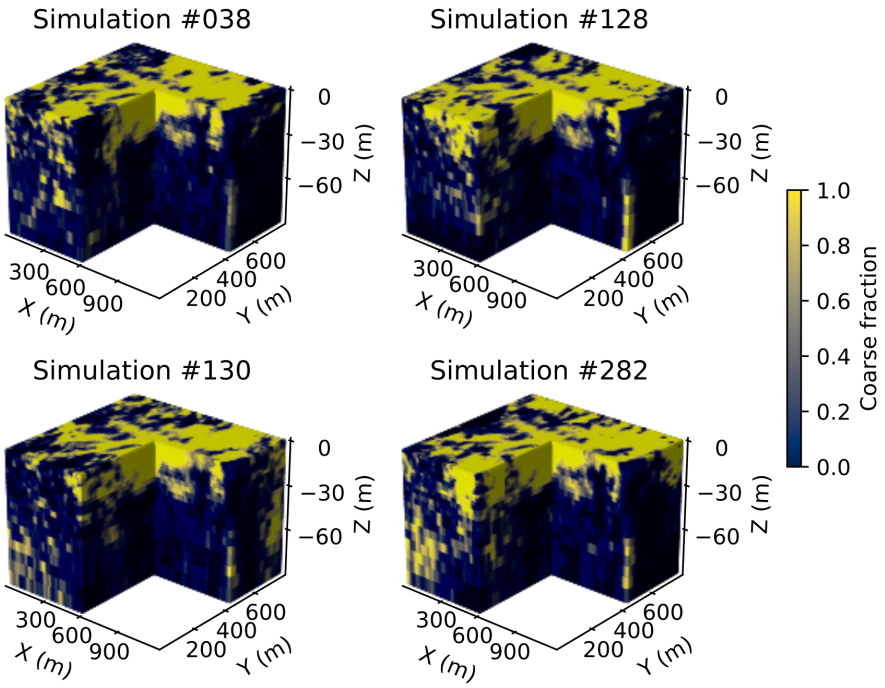


**Figure S4.** Four example coarse fraction realizations generated using the workflow described in the main text. Each realization extends from 0 to 90 m depth and is shown with 10x vertical exaggeration.

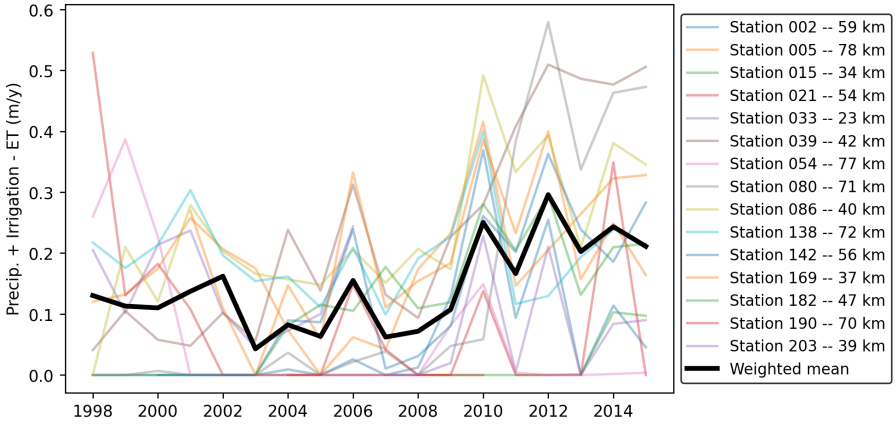


**Figure S5.** Annual net recharge rate from a hypothetical Central Valley almond orchard, using precipitation and reference evapotranspiration data from the 15 nearest CIMIS (California Irrigation Management Information System) stations to the field site. The black line is the weighted mean of individual rates calculated from each station, with stations weighted according to their proximity to the site. The legend includes each station number, as well as its distance from the field site in kilometers.

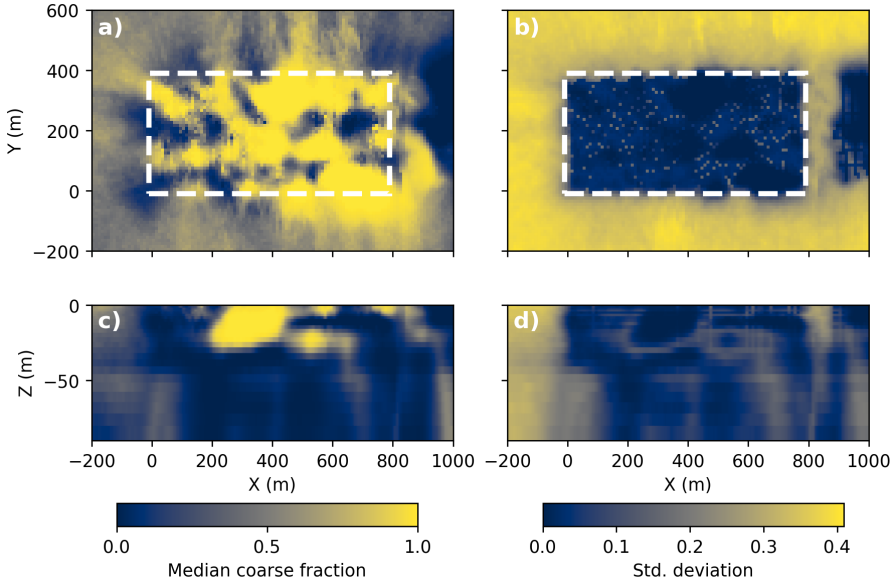


**Figure S6.** The median (a, c) and standard deviation (b, d) of coarse fraction across all 600 stochastic realizations. The top two subplots (a, b) show a top-down view of the surface layer of model cells, while the bottom two plots (c, d) show a vertical cross-section through the domain at $x$ = 200 m. The white rectangle indicates the bounds of the almond orchard.

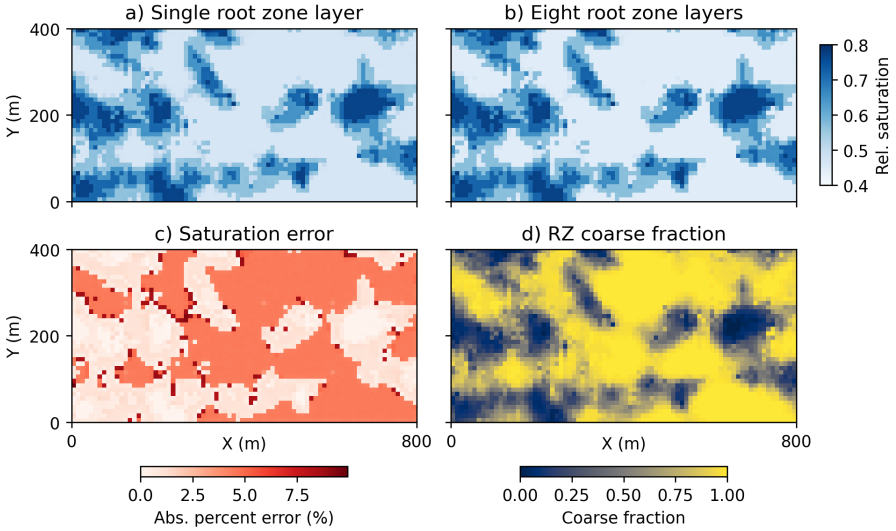


**Figure S7.** Mean root zone saturation for 14 days following inundation in (a) a simulation that represents the root zone as a single, meter-thick layer and (b) the equivalent simulation re-run with the root zone discretized into 8 separate layers (in order from top to bottom: 0.05, 0.05, 0.15, 0.15, 0.15, 0.15, 0.15, and 0.15 m). Comparing a map of absolute saturation percentage error (c) to the map of root zone coarse fraction (d) shows that the highest error values are concentrated in coarse-grained sediments.

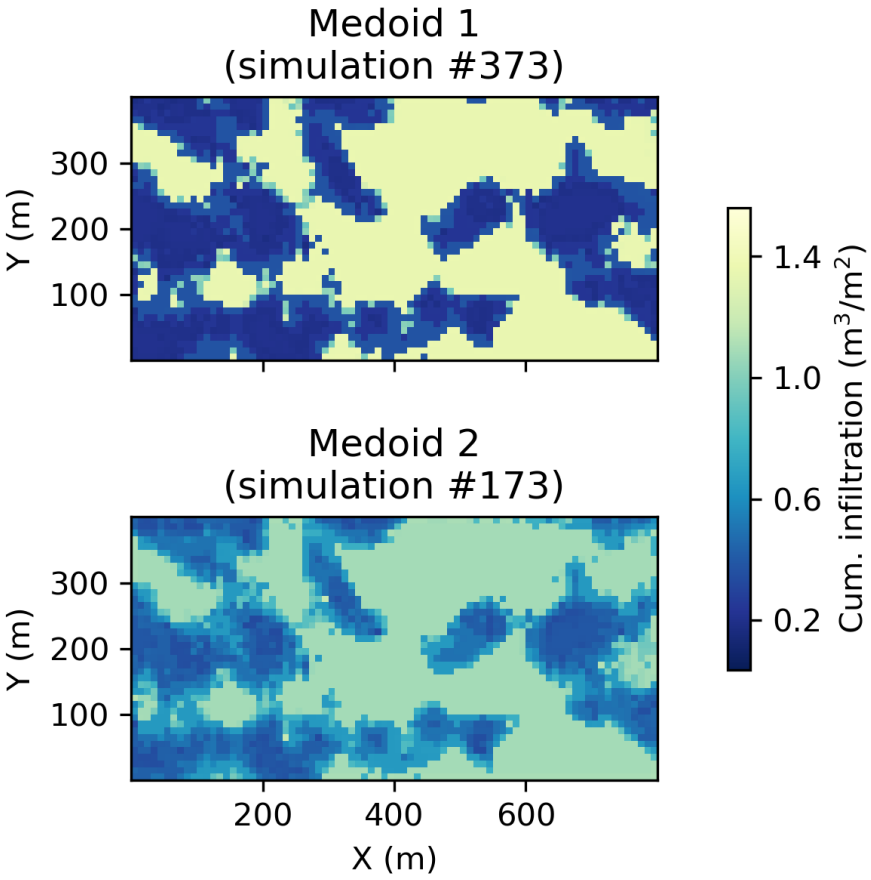


**Figure S8.** Cumulative infiltration maps for the medoids of the two clusters identified through *k*-medoids clustering. Maps only include surface cells within the bounds of the almond orchard because adjacent surface cells were not inundated.

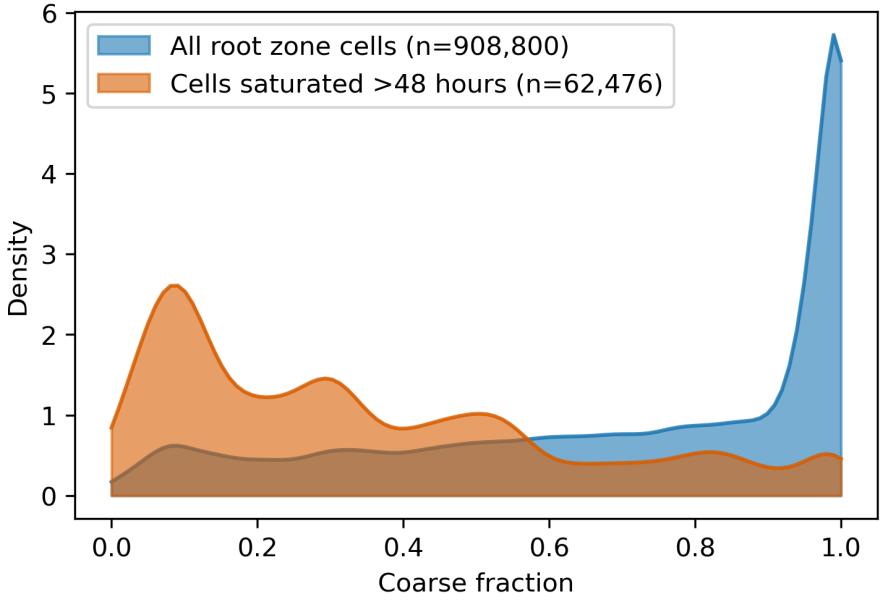


**Figure S9.** Probability density function of the coarse fraction of all root zone cells across all simulations (blue) and the conditional probability density function of the coarse fraction of cells saturated longer than 48 hours (orange). Probability density functions were generated from empirical distributions using Gaussian kernel density estimation. The legend specifies the number of cells included in each distribution. Since root zone coarse fraction varies from one simulation to another, we compute each curve across all simulations, meaning that the prior distribution (blue) includes 908,800 cells (3,200 cells per simulation across 284 simulations).

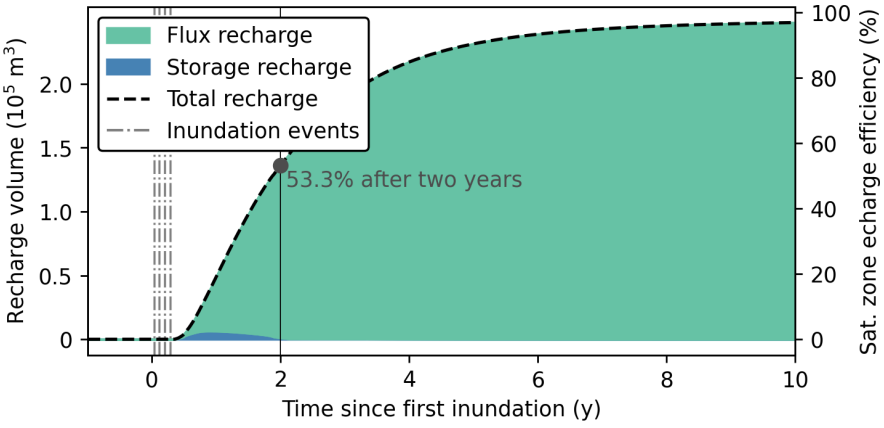


**Figure S10.** Temporal changes in the two components of recharge efficiency — storage recharge (blue) and flux recharge (green) — for a single simulation for 10 years following inundation. Flux recharge is cumulative over time, while storage recharge is transient. The recharge efficiency of this simulation is 53.3% after two years (vertical solid line) and, though recharge volume continues to increase beyond two years, it plateaus near 95%.